A New Intermolecular Potential Model for the *n*-Alkane Homologous Series

Jeffrey R. Errington and Athanassios Z. Panagiotopoulos*

School of Chemical Engineering, Cornell University, Ithaca, New York 14853, and Institute for Physical Science and Technology and Department of Chemical Engineering, University of Maryland, College Park, Maryland 20742

Received: March 22, 1999

A new model for the *n*-alkane homologous series has been developed, parametrized to the vapor−liquid coexistence properties for a range of chain lengths. The model utilizes the Buckingham exponential-6 potential to describe the nonbonded interaction energy. Histogram reweighting grand canonical Monte Carlo methods were used to determine the model parameters. The new model reproduces the experimental saturated liquid and vapor densities and vapor pressures for ethane through octane to within average absolute deviations of 0.5%, 2.1%, and 2.2% respectively. Critical temperatures and densities were also found to be in good agreement with experiment. Critical pressures are slightly overestimated for longer chain lengths. Comparisons were made to the TraPPE [*J. Phys. Chem. B* **1998**, *102*, 2569.] and NERD [*J. Chem. Phys.* **1998**, *108*, 9905.] models. The two previous models reproduce the liquid properties with comparable accuracy to the proposed model; however, the new model was found to describe the vapor pressures more accurately. Liquid densities were determined for the new model for chain lengths as long as C_{78}. Agreement to experiment is within 1% at atmospheric pressure. Phase diagrams were calculated for mixtures of ethane−heptane, ethane−decane, ethane−eicosane, and octane−dodecane. The new model achieves near-experimental predictive accuracy for these mixtures.

Introduction

Hydrocarbon molecules are important for both biological systems and the chemical industry. For example, in biological systems the side chains of several amino acids, the building blocks for proteins, consist of alkyl groups. Fatty acids are carboxylic acids with hydrocarbon chains of 4 to 36 carbons. They are the building blocks for lipids, which aggregate in an aqueous medium to form micelles and bilayers, structures related to liposomes and cell membranes. Industrially, hydrocarbons are used as feedstock for the production of natural gas, petrochemicals, gasoline, kerosene, oil, and paraffin wax. They are utilized as intermediates or solvents in the manufacturing of many products and are the building blocks for synthetic polymers.

Recent advances in simulation techniques have allowed calculation of phase equilibria of complex systems from atomistic models of the intermolecular interactions. Potential models have been proposed for a wide range of components.[1−6] Many potential models have been parametrized to liquid densities and heats of vaporization at atmospheric conditions. Such models do not give a satisfactory description of thermodynamic properties away from the state points at which they were parametrized[7]. For an accurate description of phase behavior over a broad range of temperatures, it is necessary to develop new models.

The simplest of hydrocarbons are the *n*-alkanes, which are flexible linear chains of methylene groups terminating at both ends with a methyl group. Many other classes of organic molecules, such as alkanols, amines, ketones, and carboxylic acids, are formed from the addition of functional groups to the alkane backbone. A logical starting place for development of intermolecular potential models for the phase behavior of real fluids is thus the *n*-alkane series.

There have been several previous studies aimed at developing such potential models. A common approach has been to use a "united-atom" description in which the molecules are separated into methyl and methylene groups, with an interaction site placed at each of the carbon centers. The Lennard−Jones 12-6 potential has been frequently used to describe the nonbonded energy of interaction between united atoms. For example, Laso et al. examined the phase behavior of *n*-alkanes up to pentadecane[8] using a model first proposed by de Pablo et al.[9] Siepmann, Karaborni, and Smit investigated the phase behavior of *n*-alkanes with as many as 48 carbon centers.[7,10,11] Siepmann et al. showed that the OPLS model[2] significantly overpredicts the critical temperatures of longer *n*-alkanes and that the de Pablo model,[9] although closer to the experimental value, overestimates the critical temperatures as well.[7] Subsequently, Siepmann et al. introduced the SKS model,[7] which results in critical temperatures for long *n*-alkanes that are in better agreement with experimental data. Most recently, Martin et al. and Nath et al. have introduced the most accurate models currently available, TraPPE[12] and NERD.[13] Both reproduce well the critical parameters and saturated liquid densities of *n*-alkanes over a wide range of chain lengths. However, the models are less accurate for the saturated vapor densities and vapor pressures.

An alternative to the united atom description is the more realistic all-atom representation.[14] With an all-atom model, interaction sites are placed at each of the carbon and hydrogen centers. This increases the number of interaction sites by approximately a factor of 3, which in turn increases the computational demand by roughly an order of magnitude. Although these models are computationally more intense, it is expected that the increased level of detail is necessary to successfully describe dense liquids and the solid phase of

* Author to whom correspondence should be addressed. E-mail: thanos@ipst.umd.edu.

10.1021/jp990988n CCC: $18.00
Published on Web 07/09/1999

alkanes. In addition, these models may be required to correctly describe transport properties. Chen et al.[15] have studied the phase behavior for a variety of existing all-atom models.

In this work, we propose a new united-atom model for the *n*-alkane homologous series. Our approach differs from previous work in two ways. The first is that we use the Buckingham exponential-6 potential to describe the nonbonded interaction energy. It has been shown elsewhere[16] that the added flexibility of the exponential-6 potential is needed to correctly describe the liquid and vapor properties of a relatively simple molecule like methane using a united-atom model. The expontial-6 potential has also been used with water models to obtain an improved description of the thermodynamic[17] and structural[18] properties of water.

The second difference in our approach is the use of histogram reweighting techniques to fit the model parameters. Previously, the Gibbs ensemble method has been used to determine coexisting densities and vapor pressures for a trial parameter set. While the Gibbs ensemble is a powerful tool that is useful for a wide range of applications it has drawbacks for fitting potential parameters. In particular, the uncertainty in the vapor pressure and vapor density is usually around 10%. In comparison, the vapor pressure and vapor density are calculated to within less than a percent using histogram reweighting. This allows one to fine-tune the parameters such that both the liquid and vapor properties are reproduced to a high level of accuracy. The drawback of histogram reweighting is that the process takes longer because multiple runs are needed to cover the range of temperatures and densities relevant for determining a complete coexistence curve. However, we feel that the added computational time is justified when determining potential parameters.

This paper is organized as follows. We first describe the models used and the approach for determining the new *n*-alkane model potential parameters. We then describe the simulation techniques used to calculate the properties of interest. Next, results are presented for the new model and comparisons are made to the TraPPE and NERD models. In particular, coexisting densities and vapor pressures were determined for pure components as well as liquid densities for long chains. In addition, mixture calculations were performed for ethane−heptane, ethane−decane, ethane−eicosane, and octane−dodecane systems.

Model Development

Each of the models used in the present study incorporates a united-atom description of the molecules. The nonbonded interactions between groups on different molecules and groups belonging to the same molecule separated by more than three bonds are described by a pairwise additive intermolecular potential. The NERD and TraPPE models utilize the Lennard−Jones 12-6 intermolecular potential

$$u(r) = 4\epsilon\left[\left(\frac{\sigma}{r}\right)^{12} - \left(\frac{\sigma}{r}\right)^{6}\right] \tag{1}$$

where ϵ and σ are the Lennard−Jones energy and size parameters respectively, and r is the separation distance between groups. The new model employs the Buckingham exponential-6 intermolecular potential[19]

$$u(r) = \begin{cases} \dfrac{\epsilon}{1-6/\alpha}\left[\dfrac{6}{\alpha}\exp\left(\alpha\left[1-\dfrac{r}{r_m}\right]\right) - \left(\dfrac{r_m}{r}\right)^6\right] & \text{for } r > r_{max} \\ \infty & \text{for } r < r_{max} \end{cases} \tag{2}$$

TABLE 1: Intermolecular Potential Parameters for the Models Studied

		methyl group			methylene group		
model	molecule	ϵ/k_B [K]	σ [Å]	α	ϵ/k_B [K]	σ [Å]	α
NERD	ethane	100.6	3.825				
	propane	102.6	3.857		45.8	3.93	
	n-alkane	104.0	3.91		45.8	3.93	
TraPPE	*n*-alkane	98	3.75		46	3.95	
new	*n*-alkane	129.6	3.679	16	73.5	4.00	22

where ϵ, r_m, and α are exponential-6 parameters. Parameter r_m is the radial distance at which the exponential-6 potential is a minimum. The cutoff distance r_{max} is the smallest positive value for which $du(r)/dr = 0$ and is obtained by iterative solution of eq 2. The reason a cutoff distance is required is that, at very short distances, the original Buckingham exponential-6 potential becomes negative. While canonical-ensemble Monte Carlo or molecular dynamics simulations never sample the unphysical attractive region, this is not the case on trial insertions in grand canonical simulations. The radial distance for which $u(r) = 0$, denoted by σ, can also be computed from eq 2. Again, r is the separation distance between groups. The same combining rules are used for both the Lennard−Jones 12-6 and exponential-6 potentials.

$$\sigma_{ij} = \frac{1}{2}(\sigma_{ii} + \sigma_{jj}) \tag{3}$$

$$\epsilon_{ij} = \sqrt{\epsilon_{ii}\epsilon_{jj}} \tag{4}$$

$$\alpha_{ij} = \sqrt{\alpha_{ii}\alpha_{jj}} \tag{5}$$

The nonbonded parameters for each model are summarized in Table 1.

For the NERD model, the bond lengths are generated according to the stretching potential

$$u_{stretch}(r) = \frac{K_r}{2}(r - r_{eq})^2 \tag{6}$$

with $K_r = 96500$ K/Å^2 and $r_{eq} = 1.54$ Å. The bond lengths are fixed at a value of 1.54 Å for the TraPPE model. The bond lengths are also fixed in the new model; however, the length of the bond depends on the groups being connected. The CH_3-CH_3, CH_3-CH_2, and CH_2-CH_2 bond lengths are set to 1.839, 1.687, and 1.535 Å, respectively. The bond bending angles for all of the models are generated according to the bending potential[20]

$$u_{bend}(\theta) = \frac{K_\theta}{2}(\theta - \theta_{eq})^2 \tag{7}$$

with $K_\theta = 62500$ K/rad^2 and $\theta_{eq} = 114°$. In each case, the torsion angles are described by the potential,

$$u_{tor}(\phi) = V_0 + \frac{V_1}{2}(1 + \cos\phi) + \frac{V_2}{2}(1 - \cos 2\phi) + \frac{V_3}{2}(1 + \cos 3\phi) \tag{8}$$

The parameters for the new model were taken from Smit et al.,[7] with $V_0 = 0$, $V_1 = 355.03$ K, $V_2 = -68.19$ K, and $V_3 = 791.32$ K. The Fourier coefficients for the TraPPE and NERD models are twice that of the new model, $V_0 = 0$, $V_1 = 710.06$ K, $V_2 = -136.38$ K, and $V_3 = 1582.64$ K^2.

The development of the new model started with ethane. Ethane contains two methyl groups and no methylene groups, thus allowing us to directly find suitable parameters for the methyl group. Hamiltonian scaling grand canonical Monte Carlo[16] was used to find the thermodynamic behavior of an array of diatomic exponential-6 potentials. We first tried a set of potentials with the bond length equal to the experimental C−C distance in ethane (1.536 Å). We could not find a set that simultaneously matched the coexisting densities, vapor pressures, and critical parameters. We relaxed this constraint and found an optimum value for the separation between methyl groups of 1.839 Å. We attribute the extra distance to the projection of the hydrogens along the C−C axis, causing the distance between methyl groups to be longer than the C−C bond distance. The CH_3-CH_2 distance for subsequent model development was set to $(1.839 + 1.536)/2 = 1.687$ Å.

The parameters for the methylene group were obtained from data for hexane and propane. The critical properties and coexisting densities were calculated for a given set of methylene group parameters. Hamiltonian scaling grand canonical Monte Carlo methods[16] were found to be useful in making a quick transition from one parameter set to the next. As an illustration of how this was implemented, imagine a previously examined model (model 1) with methylene parameters ϵ_1 and σ_1. It is desired to increase the value of σ while keeping the critical temperature of the model fixed at the experimental value by changing the value of ϵ. A run would be completed, with model 1 and three trial potential models, at the critical temperature of model 1. The three trial models would all have a new value of the size parameter, σ_2, with different values for the energy parameter, ϵ_{2a}, ϵ_{2b}, and ϵ_{2c}. The values of the energy parameter would be selected such that the critical temperatures of the three trial models bracketed the experimental critical temperature. The appropriate value of ϵ would then be determined from a linear interpolation of the three trial potential models. This allowed us to select a new set of parameters that would reproduce the experimental critical temperature to within a few K.

Methods

Phase Behavior of Pure Components. The phase behavior of select *n*-alkanes was determined using histogram reweighting grand canonical Monte Carlo.[21−23] A series of grand canonical simulations[24] were completed at state points in the vicinity of the coexistence curve. During the simulations a histogram was collected of observing the system with a given particle number and energy. The sequence of runs started by collecting a histogram at near critical conditions. Histogram reweighting was then used to determine the coexisting densities and activities ($\zeta = \exp(\beta\mu)/q(T)$, where $q(T)$ is the partition function of the fluid at temperature T) over a limited temperature range. To increase the temperature range over which the coexistince properties could be calculated, second and third runs were completed at a temperature of $T = T_c - \Delta T$ and at activities of $\zeta = \zeta_{coex} \pm 0.1$, where ζ_{coex} was the activity that gave phase coexistence. This corresponds to a liquid and vapor region just outside the phase envelope. The temperature increment, ΔT, was set to 35 K for ethane, 40 K for propane, butane, pentane, and hexane, and 50 K for octane and dodecane. The three histograms were combined using the techniques of Ferrenberg and Swedsen[22] and again, the coexisting densities and activities were calculated. The process was repeated for temperatures of $T_c - 2\Delta T$, $T_c - 3\Delta T$ and $T_c - 4\Delta T$. In addition, a run was completed at the critical temperature with an activity which produced a histogram with a maximum at one particle.

For each of the molecules studied the volume of the simulation box was selected such that the critical density of the given *n*-alkane corresponded to approximately 50 particles. To ascertain the effect of system size on the critical parameters, various system sizes were used to determine the critical temperature and density for ethane and octane. For each state point, five separate simulations were run. The thermodynamic properties were calculated for each set of simulations and the uncertainties were taken as the standard deviation of the five sets. The long-range corrections were calculated using the method of Theodorou and Suter.[25]

During the course of the simulation configurational bias techniques[26−29] were used for creation and anhilation of the chains as well as for molecular regrowths to change the internal structure of the chain. To increase the efficiency of these moves an early rejection scheme[30] was implemented. When growing a chain using configurational bias the creation of the molecule was split into N_{CB} steps. To implement early rejection the N_{CB} steps were divided into N_{ER} steps. An early rejection step consisted of growing a set of interaction sites using standard configurational bias. The step was then accepted with probability,

$$P = \min\left[1, W\left(\frac{\zeta V}{N+1}\right)^{1/N_{ER}}\right] \tag{9}$$

where W is the configurational bias rosenbluth factor, ζ is the activity (see definition above), V is the volume of the simulation cell, and N is the number of molecules in the system. The creation move was terminated when one of the early rejection steps failed. If all the early rejection steps were successful, then the move was accepted. The anhilation and regrowth steps were performed in an analogous manner.

The degree to which the early rejection scheme increased the efficiency of the simulation varied widely depending on the state of the fluid being simulated. At near critical conditions the early rejection scheme increased the efficiency of the transfer moves by about a factor of 3. The relative efficiency of the scheme decreased with an increase in density. It was found that the scheme was advantageous at moderate liquid densities; however, at high liquid densities the early rejection scheme was no longer beneficial. As the density of the fluid increased, the probability of a given early rejection step being accepted decreased. Eventually, the probability of accepting N_{ER} successive early rejection steps became too low compared to the probabilty of growing the complete chain in one step to make the scheme useful.

P−V−T Properties of *n*-Alkanes. The isothermal−isobaric ensemble[31] was used to determine the densities of chains with 11 to 78 carbon atoms. The simulations consisted of translation, rotation, volume change, configurational bias regrowth, and concerted rotation[32] moves. Configurational bias regrowths were useful for changing the configuration toward the end of the chains; however, moves that originated deep in the interior of a long chain were rarely accepted. As a result, the concerted rotation move was added to ensure that the internal stucture of the entire chain was adequately sampled. The concerted rotation move displaces four of the internal methylene groups at a time while keeping the rest of the chain in place. The number of molecules used in each simulation depended on the length of the chain, with the number of molecules set such that the simulation cell consisted of approximately 2400 interaction sites.

Mixture Calculations. The constant pressure Gibbs ensemble[33−35] was coupled with expanded ensemble techniques[36] to calculate mixture phase coexistence. The simulations

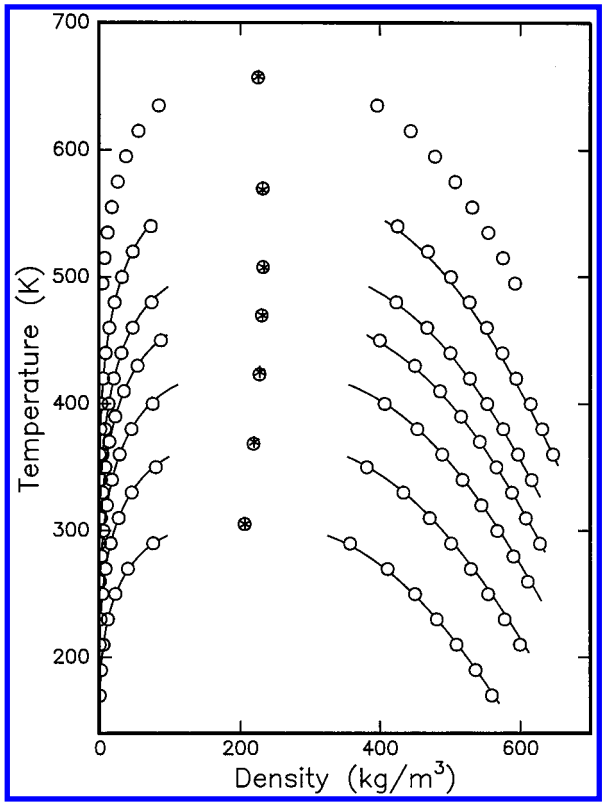

Figure 1. Phase diagram of select *n*-alkanes. The curves from bottom to top are for ethane, propane, butane, pentane, hexane, octane, and dodecane. The circles represent calculations for the new model. Uncertainties are smaller than the size of the symbols. A solid line is used for experimental data and an asterisk for the experimental critical point. Please refer to the text for the source of the experimental data.

consisted of translation, rotation, volume change, configurational bias regrowth, and transfer moves. A total of 300 molecules were used for the ethane−heptane, ethane−decane, and ethane−eicosane systems. A total of 200 molecules were used for the octane−dodecane mixture.

Results and Discussion

Phase Behavior of Pure Components. The coexisting densities of select *n*-alkanes predicted by the new model are compared to experimental values in Figure 1. The experimental coexisting densities for ethane, propane, and butane were obtained from the NIST Chemistry WebBook,[37] whereas the values for pentane, hexane, and octane were taken from the compilation of Smith and Srivastava.[38] The experimental critical parameters were obtained from a review compiled by Ambrose and Tsonopoulos.[39] The uncertainties of the simulated points are less than the size of the symbol. Complete data sets are available as Supporting Information from the author.[40] Overall agreement between the model and experimental data is quite good. The model reproduces the experimental saturated liquid densities for ethane through octane to within an average error of 0.5% and the saturated vapor densities to within 2.1%.

The vapor pressures of the new model are presented in Figure 2. Again, the agreement between the model and experimental data is quite good, with the model reproducing the experimental vapor pressures for ethane through octane to within an average error of 2.2%. For the smaller molecules the change in the vapor pressure with temperature, or the heat of vaporization, is in good agreement with experiment. As the chain length increases, the slope of the vapor pressure curve predicted by the model becomes slightly greater than experimentally observed. For

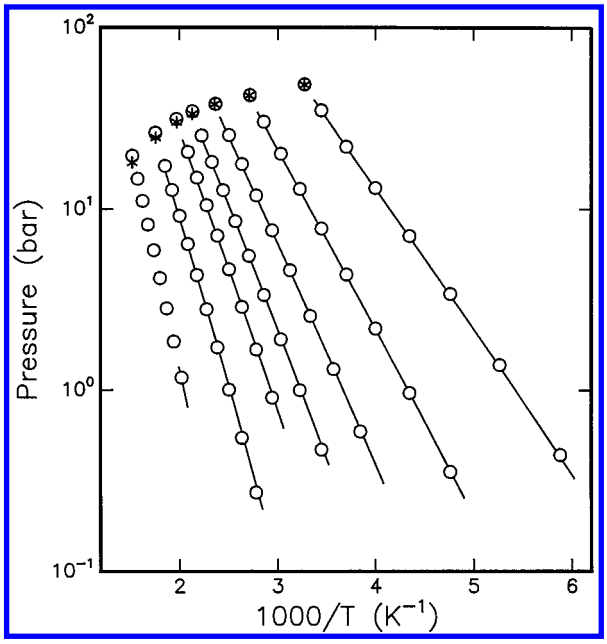

Figure 2. Vapor pressure of select *n*-alkanes. The curves from right to left are for ethane, propane, butane, pentane, hexane, octane, and dodecane. Symbols are the same as in Figure 1.

example, the critical pressure of octane is overpredicted by 6%, whereas the vapor pressure at the lowest temperature simulated, 360 K, is underestimated by 9%. It is not clear if this is due to the united-atom representation or to the specific parameters chosen.

The coexistence and vapor pressure curves of ethane are shown in Figure 3. The coexistence properties calculated in this study for the TraPPE and NERD models are in very good agreement with previously reported values by Martin et al.[12] and Nath et al.[13] The TraPPE and new models accurately reproduce the saturated liquid densities, however the NERD model underestimates the liquid densities at low temperatures. The NERD model also overestimates the critical temperature by 7 K. Both the NERD and new models correctly describe the vapor pressure of ethane; however, the TraPPE model consistently overestimates the vapor pressure with the deviation from experiment greatest at lower temperatures, reading 65% error at 160 K. The major difference between the new model and the TraPPE and NERD models is the separation distance between the methyl groups. We have found that it is impossible to reproduce the coexisting densities, vapor pressure, and critical behavior of ethane simultaneously using the experimental C−C bond length for the separation distance between methyl groups. If the experimental C−C bond length is used the vapor pressure has to be sacrificed in favor of the liquid densities and critical parameters, or the critical temperature and liquid densities at low temperatures must be forfeited in favor of correct vapor pressures.

The coexistence and vapor pressure curves of octane are displayed in Figure 4. It is clear that all three models adequately reproduce the saturated liquid densities and critical point. Differences between the three models are observed in their description of the vapor pressure. Both the TraPPE and NERD models overestimate the vapor pressures over the entire temperature range, with the NERD model being closer to experimental values. The new model overestimates the vapor pressure at high temperatures and underestimates at low temperatures, with the new model in better overall agreement with experimental data over the entire temperature range. Although the slope of the vapor pressure curves, or heats of vaporization, for

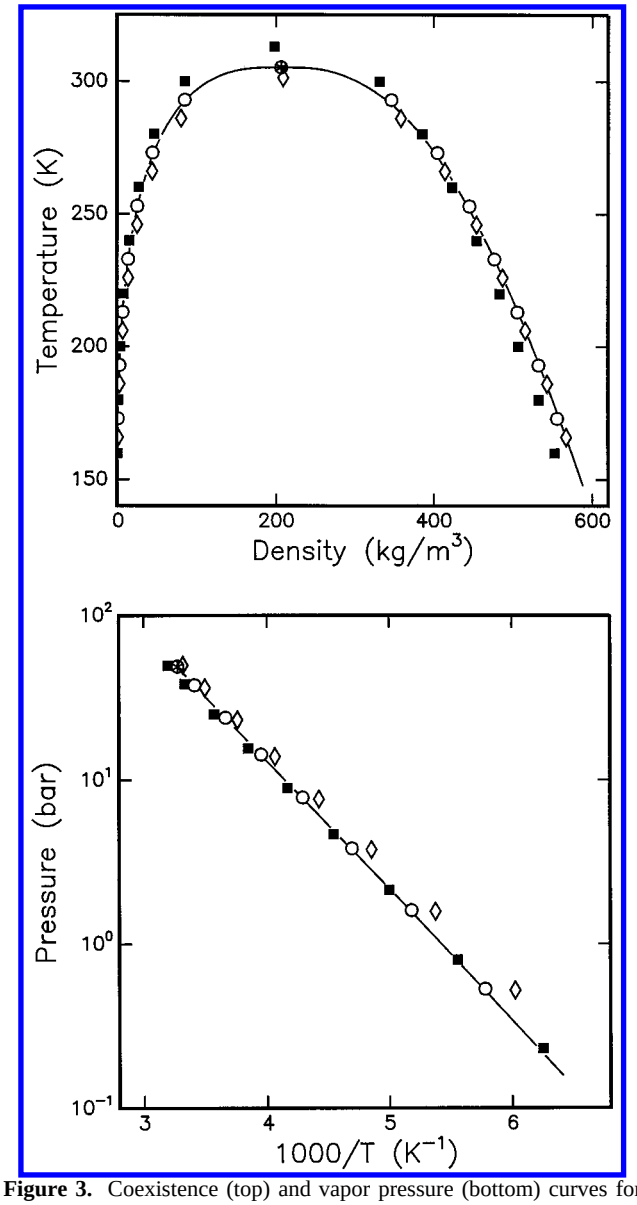

Figure 3. Coexistence (top) and vapor pressure (bottom) curves for ethane. Squares, diamonds, and circles are used to represent the NERD, TraPPE, and new models, respectively. Uncertainties are smaller than the size of the symbols. A solid line is used for experimental data.

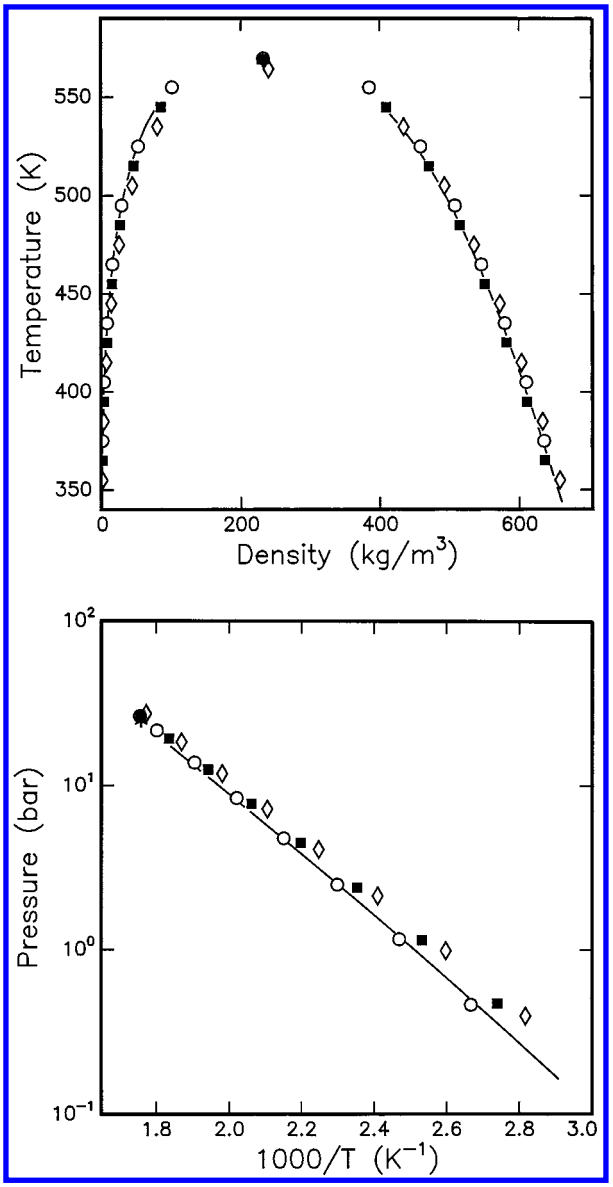

Figure 4. Coexistence (top) and vapor pressure (bottom) curves for octane. Symbols are the same as in Figure 3.

all three of the models are reasonable, none of the models precisely reproduces the heat of vaporization of octane. For example, at 450 K the values of the heat of vaporization for the NERD, TraPPE, and new model are 32.5, 31.6, and 36.3 kJ/mol respectively, whereas the experimental value is 34.4 kJ/mol.[38]

The critical parameters of the models are presented in Table 2. The critical temperatures and densities were found from a mixed-field analysis[41−43] on histograms that were collected during grand canonical Monte Carlo runs at near critical conditions. The critical pressures were calculated by extrapolating the vapor pressure curve, found using histogram reweighting,[16] to the critical temperature. The volume of a simulation cell was chosen such that the critical density corresponded to approximately 50 particles. The uncertainties listed for the critical parameters are merely the statistical uncertainties obtained from a single system size. To ascertain the effect of system size on the critical parameters various system sizes were used to determine the critical temperature and density for ethane and octane. Grand canonical runs were completed at critical conditions with volumes of one-half and twice the original volume. For ethane an additional run was completed with a simulation cell four times the original volume. The results are tabulated in Table 3. The effect of system size on the critical temperature is shown in Figure 5. The infinite system size parameters were extrapolated using finite-size scaling.[41−43] We did not feel that the smallest system sizes used fell into the scaling regime and therefore did not use these points in the infinite system size extrapolation. For ethane the critical temperature and density at infinite system size both differ by 1.0% from the system size used to parametrize the model. For octane, the difference is 0.3% and 0.7% respectively. The effect of system size on the simulated thermodynamic properties is most pronounced in the near critical region. The change in the simulated thermophysical properties away from the near critical region is within simulation uncertainties.

The critical temperature, density, and pressure as a function of chain length are shown in Figures 6, 7, and 8, respectively. All of the models adequately predict the critical temperatures over the range of chain lengths studied. Differences between the three models are observed in the description of the critical density. For shorter chain lengths the TraPPE model tends to overestimate the critical density, whereas the NERD model

TABLE 2: Critical Parameters of the Models Studied

molecule	model	T_c (K)	ρ_c (kg/m^3)	p_c (bar)	Z_c
ethane	NERD	313.0 ± 0.4	197.6 ± 1.0	49.5 ± 0.4	0.290 ± 0.002
	TraPPE	301.4 ± 0.5	208.8 ± 0.8	49.8 ± 0.5	0.286 ± 0.002
	new	305.3 ± 0.6	206.2 ± 0.8	49.0 ± 0.6	0.282 ± 0.002
	expt	305.3	206.6	48.72	0.279
propane	new	368.4 ± 0.4	218.8 ± 0.6	42.7 ± 0.3	0.281 ± 0.002
	expt	369.8	220	42.5	0.277
butane	new	423.3 ± 0.4	227.5 ± 1.0	38.2 ± 0.4	0.278 ± 0.003
	expt	425.1	228	38.0	0.274
pentane	NERD	476.9 ± 0.8	227.4 ± 0.8	34.9 ± 0.4	0.278 ± 0.003
	TraPPE	464.2 ± 0.4	238.9 ± 1.8	35.9 ± 0.3	0.282 ± 0.003
	new	469.7 ± 0.4	230.7 ± 0.8	34.8 ± 0.3	0.279 ± 0.002
	expt	469.7	232	33.7	0.268
hexane	new	507.9 ± 0.7	232.6 ± 1.6	31.6 ± 0.5	0.277 ± 0.004
	expt	507.6	234	30.3	0.264
octane	NERD	569.2 ± 1.2	231.2 ± 2.9	26.7 ± 0.4	0.278 ± 0.004
	TraPPE	564.3 ± 1.6	240.3 ± 3.1	27.4 ± 0.5	0.278 ± 0.006
	new	569.7 ± 0.8	232.3 ± 0.8	26.5 ± 0.3	0.276 ± 0.002
	expt	568.7	232	24.9	0.259
dodecane	new	657.1 ± 1.0	225.2 ± 1.4	19.8 ± 0.3	0.274 ± 0.003
	expt	658	226	18.2	0.251
hexadecane	new	719.5 ± 1.2	217.2 ± 1.6	15.2 ± 0.3	0.264 ± 0.004
	expt	723	219	14.0	0.241
tetracosane	new	803.5 ± 1.2	201.8 ± 2.0	10.3 ± 0.3	0.259 ± 0.004
	expt	800	n. a.	8.7	n. a.
octatetracontane	new	939 ± 3	170 ± 7	5.2 ± 0.3	0.264 ± 0.010
	expt	n. a.	n. a.	n. a.	n. a.

TABLE 3: Apparent Critical Temperature and Density as a Function of System Size

molecule	V (Å^3)	N_c	T_c (K)	ρ_c (kg/m^3)
ethane	7 500	30.4 ± 0.1	304.0 ± 0.5	202.7 ± 0.5
	15 000	61.9 ± 0.2	305.3 ± 0.6	206.1 ± 0.7
	30 000	124.3 ± 0.8	306.5 ± 0.6	206.8 ± 1.3
	60 000	249.6 ± 1.3	307.4 ± 0.5	207.7 ± 1.1
	extrapolation		308.3	208.1
octane	20 000	23.9 ± 0.3	568.8 ± 0.8	227.0 ± 3.3
	40 000	49.0 ± 0.1	569.6 ± 0.7	232.2 ± 0.6
	60 000	98.3 ± 0.3	570.3 ± 0.7	233.0 ± 0.8
	extrapolation		571.1	233.8

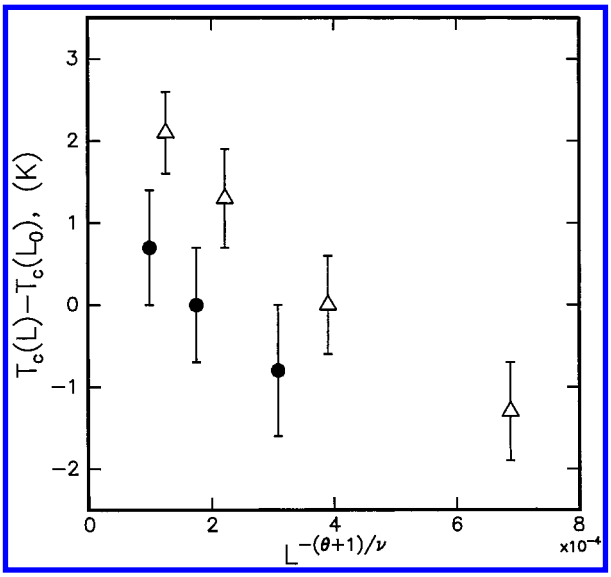

Figure 5. Deviation of the apparent critical temperature from the critical temperature at the system size used to parametrize the model. Open triangles and filled circles are used for ethane and octane, respectively. The scaling variables θ and ν have values of 0.54 and 0.629, respectively.

slightly underestimates the critical density. For longer chain lengths it is difficult to make comparisons between the models due to the increasing uncertainties of the experimental values.

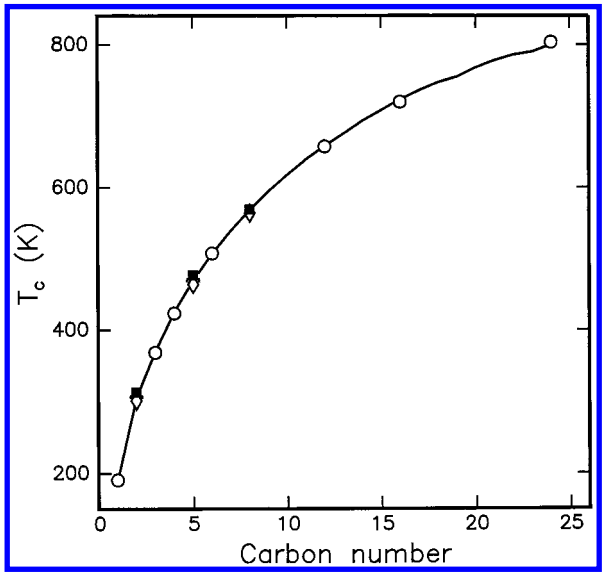

Figure 6. Critical temperature of the *n*-alkanes as a function of carbon number. Symbols are the same as in Figure 3.

An example of the uncertainty in the experimental data is shown in Figure 7 for C_7 and C_{13}. All three of the models overestimate the critical pressures, with the relative deviation from experiment increasing with increasing chain length. For example, the new model overpredicts the critical pressure of tetracosane by 15%. In general, the NERD and new models tend to be slightly closer to experimental values than the TraPPE model. Nath et al. have reported critical temperatures and densities for the NERD model for chain lengths as long as C_{48}.[13] It is interesting to note that although the reported value for the critical temperature of C_{24} for the NERD model and our estimate for our new model are very close, the predicted values for C_{48} are significantly different. The calculated value for the new model, 939 K, is close to the value estimated from the correlation of Teja et al.,[44] whereas the value for the NERD model, 905 K, is close to the correlation of Tsonopoulos.[45] Both the NERD model and the new model predict a value for the critical density of C_{48} that is

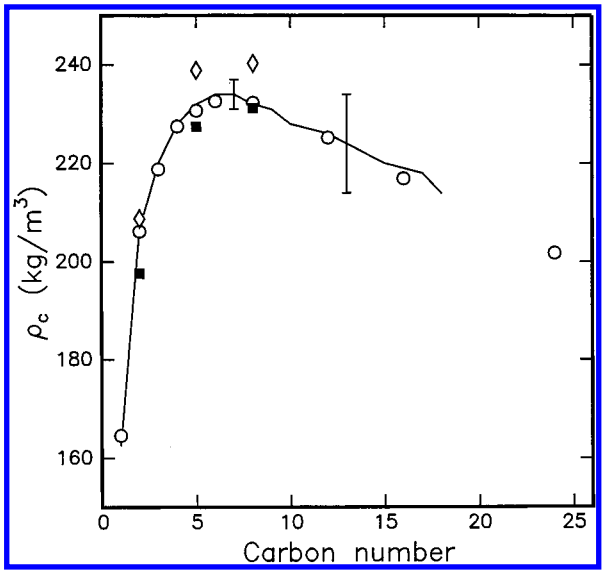

Figure 7. Critical density of the *n*-alkanes as a function of carbon number. Symbols are the same as in Figure 3. The error bars at C_7 and C_{13} represent the uncertainty in the experimental data.

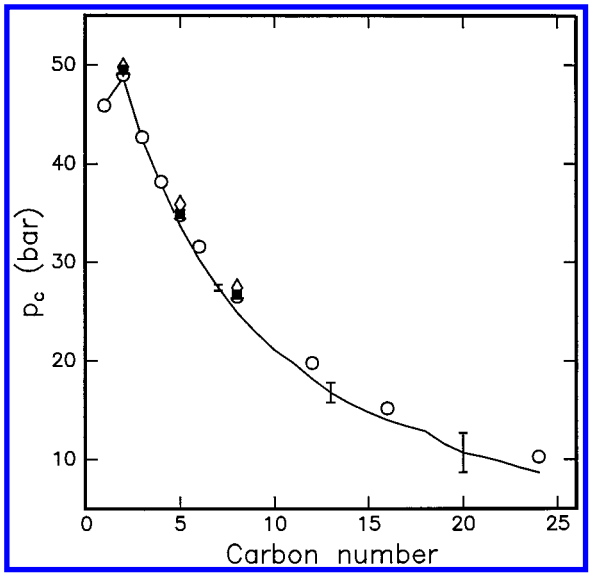

Figure 8. Critical pressure of the *n*-alkanes as a function of carbon number. Symbols are the same as in Figure 3. The error bars at C_7, C_{13}, and C_{20} represent the uncertainty in the experimental data.

TABLE 4: Results of *NpT* Simulations

chain length	no. of molecules	T (K)	P (bar)	ρ_{expt} (kg/m^3)	ρ_{model} (kg/m^3)
C_{11}	200	360	1	695.0	693 ± 7
	200	420	1	645.7	645 ± 2
C_{16}	150	360	1	732.1	723 ± 4
	150	420	1	689.0	686 ± 4
	150	510	1	612.0	617 ± 9
C_{24}	100	360	1	755.6	755 ± 4
	100	420	1	718.5	715 ± 3
	100	510	1	656.2	647 ± 4
C_{36}	68	420	1	739.9	738 ± 4
	68	510	1	681.9	682 ± 7
C_{44}	55	420	1	752.7	746 ± 3
	55	510	1	695.4	689 ± 6
	55	510	50	701.8	695 ± 3
	55	510	100	707.7	703 ± 4
	55	510	500	744.1	736 ± 7
	55	510	1000	775.1	763 ± 3
C_{78}	32	420	1	765.0	760 ± 4
	32	510	1	712.7	706 ± 3

in better agreement with the correlation of Teja et al. than of Tsonopoulos.

P−V−T Properties of *n*-Alkanes. Liquid densities for chain lengths as long as C_{78} are listed in Table 4. The results from calculations at atmospheric pressure are displayed in Figure 9. Agreement between experimental values[46] and the new model is very good for chains as long as C_{36}. However, the estimates for the new model are about 1% too low for C_{44} and C_{78}. Results were also obtained over a range of pressures at 510 K for C_{44}. The difference from experimental values remains at approximately 1% up to a pressure of 500 bar. The value at a pressure of 1000 bar deviates from the experimental value by slightly more, underestimating the density by 1.5%.

Mixture Calculations. The phase diagram for a mixture of ethane and heptane at 366 K is shown in Figure 10. The values for the TraPPE and NERD model were obtained from calculations done by Martin et al.[47] and Nath et al.[48] respectively. The calculations for the TraPPE model were determined using a preliminary version of the TraPPE force field. It is observed that the NERD model overestimates the liquid composition over the entire pressure range. The TraPPE model and new model are closer to experimental values,[49] with both models slightly underpredicting the liquid composition at intermediate pressures.

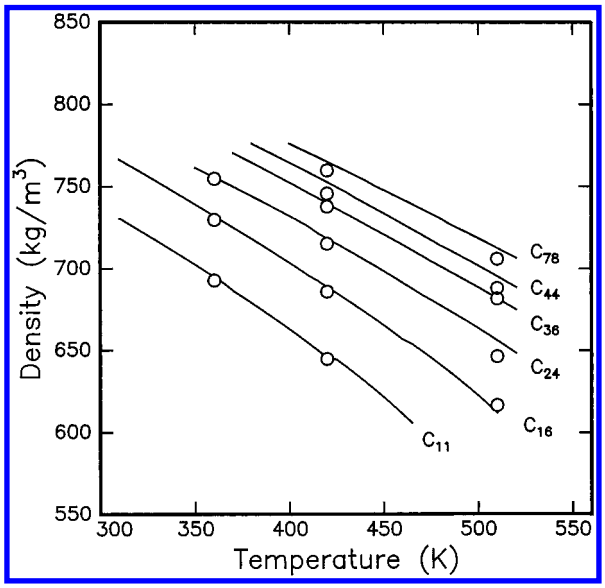

Figure 9. Liquid densities at atmospheric pressure. Circles represent the new model. Solid lines are used for experimental data.

The phase diagram for the ethane−decane system at 411 K is displayed in Figure 11. Again, the predictions for the NERD model[48] overestimate liquid compositions throughout the entire pressure range. The new model agrees with experimental data[49] to within the uncertainty of the simulation data. Figure 12 shows the results for the ethane−eicosane system at 96.526 bar. The results for the NERD model[48] follow the same trend; the liquid composition is consistently overestimated. The new model slightly underestimates the experimental liquid compositions[50] over the entire temperature range. The results for the ethane−*n*-alkane systems show that the new model can be used to reliably predict the phase coexistence of supercritical mixtures.

The boiling point diagram for the octane−dodecane system at 0.2 bar is displayed in Figure 13. The TraPPE model[47] underestimates the liquid and vapor compositions at all temperatures. This is a direct consequence of the inability of the model to correctly describe the pure component vapor pressures.

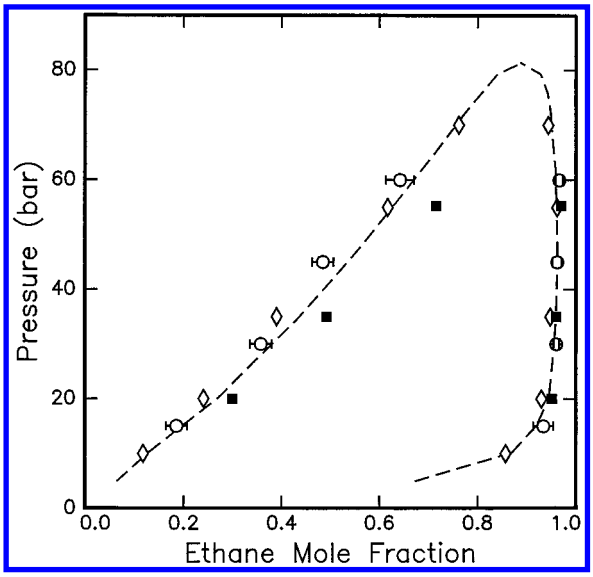

Figure 10. Phase diagram for a mixture of ethane and heptane at 366 K. Squares, diamonds, and circles are used to represent the NERD, TraPPE, and new models, respectively. A dashed line is used for experimental data.

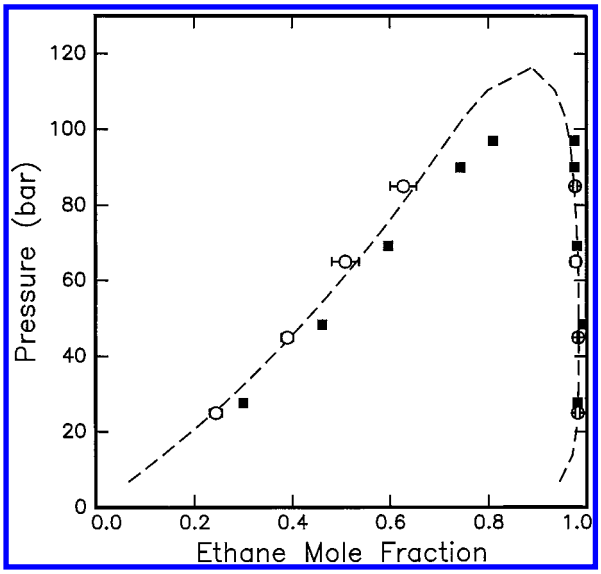

Figure 11. Phase diagram for a mixture of ethane and decane at 411 K. Symbols are the same as in Figure 10.

The new model is in better agreement with experimental values.[51]

In a forthcoming publication,[52] phase diagrams are presented for mixtures of methane and pentane, carbon dioxide with select *n*-alkanes, and methanol with select *n*-alkanes. These calculations have been completed using histogram reweighting techniques.

Conclusions

A new united-atom model for the *n*-alkane homologous series that uses the Buckingham exponential-6 potential to describe the nonbonded interactions has been developed. The model was optimized to reproduce the saturated liquid and vapor densities, vapor pressures, and critical parameters of the *n*-alkane series. Histogram reweighting techniques were used to calculate the phase coexistence properties.

Comparisons were made to the TraPPE and NERD models. It was found that all three models reproduce adequately experimental saturated liquid densities. The three models

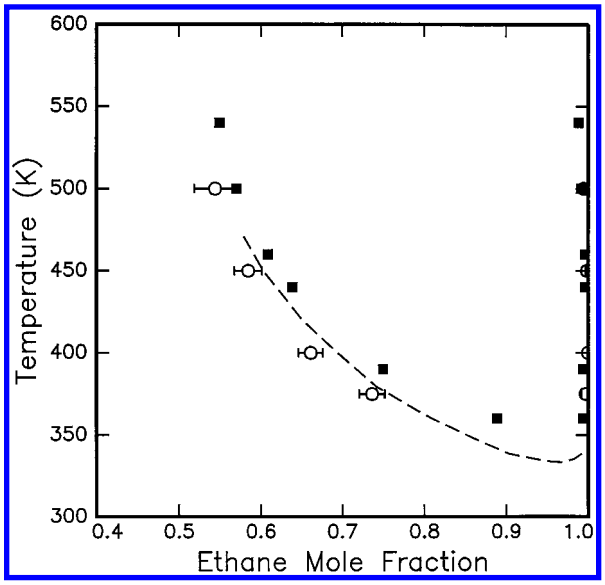

Figure 12. Phase diagram for a mixture of ethane and eicosane at 96.526 bar. Symbols are the same as in Figure 10.

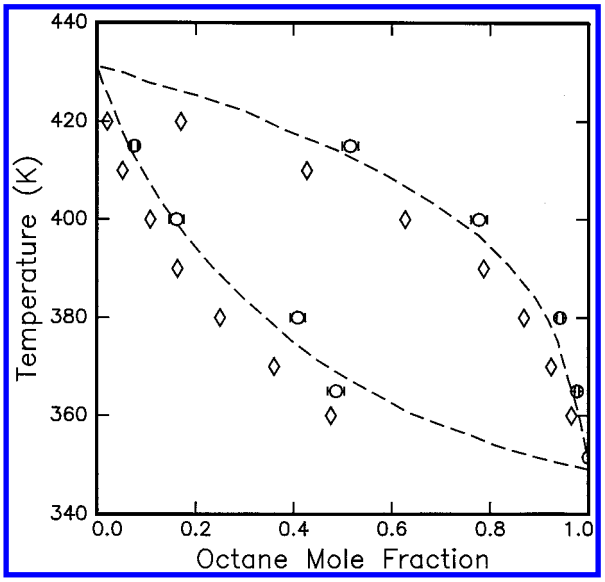

Figure 13. Phase diagram for a mixture of octane and dodecane at 0.2 bar. Symbols are the same as in Figure 10.

describe experimental vapor pressures with varying degrees of success. The TraPPE model consistently overestimated the vapor pressures, with the deviation from experiment greatest at low reduced temperatures. The NERD model exhibited similar behavior for longer chains, with the results being closer to experimental values than the TraPPE model. In general, the new model was able to reproduce the vapor pressures to a higher level of accuracy. The agreement was best for shorter chain lengths. The new model slightly overestimates the critical pressure and underestimates the vapor pressure at low reduced temperatures for longer chains. The critical parameters for the models were found to be in good agreement with experiment. The critical temperatures were reproduced most accurately, with all three models in good agreement with experiment. The critical densities were overestimated by the TraPPE model and slightly underpredicted by the NERD model. The critical pressures were overpredicted by all three of the models, with the deviation from experiment increasing with chain length. The mixture behavior for four mixtures has also been studied. The results were found to be in good agreement with experimental data. This indicates that simulations using united-atom models fit to

pure component data can be used to determine the phase behavior of complex non-polar mixtures with reasonable accuracy. The next logical step in the development of intermolecular potential models is a model for the branched alkanes. We are currently working on such a model.

Acknowledgment. Financial support for this work has been provided by the National Science Foundation, under grant CTS-9509158. We acknowledge helpful discussions with Profs. J. J. de Pablo and J. I. Siepmann, who also provided us with preprints of papers prior to publication.

References and Notes

(1) Ryckaert, J. P.; Bellemans, A. *Chem. Phys. Lett.* **1975**, *30*, 123.
(2) Jorgensen, W. L.; Madura, J. D.; Swenson, C. J. *J. Am. Chem. Soc.* **1984**, *106*, 813.
(3) Stillinger, F. H.; Rahman, A. *J. Chem. Phys.* **1974,** *60*, 1545.
(4) Berendsen, H. J. C.; Postma, J. P. M.; van Gunsteren, W. F.; Hermans, J. In *Intermolecular Forces*; Pullman, B., Ed.; Reidel: Dordrecht, Holland, 1981.
(5) Van Leeuwen, M. E.; Smit, B. *J. Phys. Chem.* **1995**, *99*, 1831.
(6) Harris, J. G.; Yung, K. H. *J. Phys. Chem.* **1995**, *99*, 12021.
(7) Smit, B.; Karaborni, S.; Siepmann, J. I. *J. Chem. Phys.* **1995**, *102*, 2126.
(8) Laso, M.; de Pablo, J. J.; Suter, U. W. *J. Chem. Phys.* **1992**, *97*, 2817.
(9) De Pablo, J. J.; Laso, M.; Siepmann, J. I.; Suter, U. W. *Mol. Phys.* **1993**, *80*, 55.
(10) Siepmann, J. I.; Karaborni, S.; Smit, B. *J. Am. Chem. Soc.* **1993**, *115*, 6454.
(11) Siepmann, J. I.; Karaborni, S.; Smit, B. *Nature* **1993**, *365*, 330.
(12) Martin, M. G.; Siepmann, J. I. *J. Phys. Chem. B* **1998**, *102*, 2569.
(13) Nath, S. K.; Escobedo, F. A.; de Pablo, J. J. *J. Chem. Phys.* **1998**, *108*, 9905.
(14) Williams, D. E. *J. Chem. Phys.* **1967**, *47*, 4680.
(15) Chen, B.; Martin, M. G.; Siepmann, J. I. *J. Phys. Chem B* **1998**, *102*, 2578.
(16) Errington, J. R.; Panagiotopoulos, A. Z. *J. Chem. Phys.* **1998**, *109*, 1093.
(17) Errington, J. R.; Panagiotopoulos, A. Z. *J. Phys. Chem. B*, **1998,** *102*, 7470.
(18) Chialvo, A. A.; Cummings, P. T. *Fluid Phase Equil.* **1998**, *150*−*151*, 73.
(19) Buckingham, R. A. *Proc. R. Soc.* **1938**, *168A*, 264.
(20) Van der Ploeg, P.; Berendsen, H. J. C. *J. Chem. Phys.* **1982**, *94*, 3271.
(21) Ferrenberg, A. M.; Swendsen, R. H. *Phys. Rev. Lett.* **1988**, *61*, 2635.
(22) Ferrenberg, A. M.; Swendsen, R. H. *Phys. Rev. Lett*. **1989**, *63*, 1195.
(23) Panagiotopoulos, A. Z.; Wong, V.; Floriano, M. A. *Macromolecules* **1998**, *31*, 912.
(24) Norman, G. E.; Filinov, V. S. *High Temp.* **1969**, *7*, 216.
(25) Theodorou, D. N.; Suter, U. W. *J. Chem. Phys.* **1985**, *82*, 955.
(26) Siepmann, J. I. *Mol. Phys.* **1990**, *70*, 1145.
(27) Siepmann, J. I.; Frenkel, D. *Mol. Phys.* **1992**, *75*, 59.
(28) Frenkel, D.; Mooij, G. C. A. M.; Smit, B. *J. Phys. Condens. Matter* **1992**, *4*, 3053.
(29) De Pablo, J. J.; Laso, M.; Suter, U. W. *J. Chem. Phys.* **1992**, *96*, 2395.
(30) Frenkel, D.; Smit, B. *Understanding Molecular Simulation*; Academic Press: London, 1996.
(31) Wood, W. W. *J. Chem. Phys.* **1968**, *48*, 415.
(32) Dodd, L. R.; Boone, T. D.; Theodorou, D. N. *Mol. Phys.* **1993**, *78*, 961.
(33) Panagiotopoulos, A. Z. *Mol. Phys.* **1987,** *61*, 813.
(34) Panagiotopoulos, A. Z.; Quirke, N.; Stapleton, M.; Tildesley, D. J. *Mol. Phys.* **1988,** *63*, 527.
(35) Smit, B.; de Smedt, P.; Frenkel, D. *Mol. Phys*. **1989,** *68*, 931.
(36) Escobedo, F. A.; de Pablo, J. J. *J. Chem. Phys.* **1996**, *105*, 4391.
(37) NIST Chemistry WebBook. http://webbook.nist.gov/chemistry.
(38) Smith, B. D.; Srivastava, R. *Thermodynamic data for pure compounds: Part A Hydrocarbons and Ketones*; Elsevier: Amsterdam, 1986.
(39) Ambrose, D.; Tsonopoulos, C. *J. Chem. Eng. Data* **1995**, *40*, 531.
(40) http://thera.umd.edu/jerring/n-alkanes.
(41) Wilding, N. B.; Bruce, A. D. *J. Phys. Condens. Matter* **1992**, *4*, 3087.
(42) Wilding, N. B. *Phys. Rev. E* **1995**, *52*, 602.
(43) Potoff, J. J.; Panagiotopoulos, A. Z. *J. Chem. Phys.* **1998**, *109*, 10914.
(44) Teja, A. S.; Lee, R. J.; Rosenthal, D.; Anselme, M. *Fluid Phase Equilibria* **1990**, *56*, 153.
(45) Tsonopoulos, C. *AIChE J.* **1987**, *33*, 2080.
(46) Dee, G. T.; Ougizawa, T.; Walsh, D. J. *Polymer* **1992**, *33*, 3462.
(47) Martin, M. G.; Siepmann, J. I. *J. Am. Chem. Soc.* **1997**, *119*, 8921.
(48) Nath, S. K.; Escobedo, F. A.; de Pablo, J. J. *Ind. Eng. Chem. Res.* **1998**, *37*, 3195.
(49) Gmehling, J.; Onken, U. *Vapor-Liquid Equilibrium Data Collection*; Chemistry Data Series; DECHEMA: Frankfurt/Main, 1997−1990.
(50) Peters, C. J.; Roo, J. L.; Lichtenthaler, R. N. *Fluid Phase Equil.* **1987**, *34*, 287.
(51) Dejoz, A.; González-Alfaro, V.; Miguel, P. J.; Vázquez, M. I. *J. Chem. Eng. Data* **1996**, *41*, 93.
(52) Potoff, J. J.; Errington, J. R.; Panagiotopoulos, A. Z. *Mol. Phys.* **1999**, in press.